REPORT DOCUMENTATION PAGE

Form Approved
OMB NO. 0704-0188

1. AGENCY USE ONLY (Leave Blank)	2. REPORT DATE	3. REPORT TYPE AND DATES COVERED
		Final report Jan 1, 2005 - 31 Dec, 2007

4. TITLE AND SUBTITLE

Electromagnetic Models and Inversion Techniques for Multiple UXO Discrimination

5. FUNDING NUMBERS

W911NF-05-1-0023

6. AUTHOR(S)

Jin Au Kong, Bae-Ian Wu, Beijia Zhang, Hongsheng Chen

7. PERFORMING ORGANIZATION NAME(S) AND ADDRESS(ES)

M.I.T
Research Laboratory of Electronics

8. PERFORMING ORGANIZATION REPORT NUMBER

9. SPONSORING / MONITORING AGENCY NAME(S) AND ADDRESS(ES)

U. S. Army Research Office
P.O. Box 12211
Research Triangle Park, NC 27709-2211

10. SPONSORING / MONITORING AGENCY REPORT NUMBER

44502.1-EV

11. SUPPLEMENTARY NOTES

The views, opinions and/or findings contained in this report are those of the author(s) and should not be construed as an official Department of the Army position, policy or decision, unless so designated by other documentation.

12 a. DISTRIBUTION / AVAILABILITY STATEMENT

Approved for public release; distribution unlimited.

12 b. DISTRIBUTION CODE

13. ABSTRACT (Maximum 200 words)

N/A

14. SUBJECT TERMS

15. NUMBER OF PAGES

22

16. PRICE CODE

17. SECURITY CLASSIFICATION OR REPORT	18. SECURITY CLASSIFICATION ON THIS PAGE	19. SECURITY CLASSIFICATION OF ABSTRACT	20. LIMITATION OF ABSTRACT
UNCLASSIFIED	**UNCLASSIFIED**	**UNCLASSIFIED**	UU

NSN 7540-01-280-5500

Standard Form 298 (Rev.2-89)
Prescribed by ANSI Std. 239-18
298-102

Electromagnetic models and inversion techniques for multiple UXO discrimination

Final report (Sponsor ID: W911NF-05-1-0023)

Jin Au Kong, Bae-Ian Wu, Beijia Zhang, Hongsheng Chen

Research Laboratory of Electronics, Massachusetts Institute of Technology, Cambridge, MA 02139, USA

Abstract

Recovery of buried unexploded ordnance (UXO) is very slow and expensive due to the high false alarm rate created by clutter. Electromagnetic induction (EMI) has been shown to be a promising technique for UXO detection and discrimination. We use the EMI response of buried targets to identify or classify them. Given that now a more complete model of the measurable response of a buried UXO is implemented, this study proceeds to demonstrate that EMI responses from UXO and clutter objects can be used to identify the objects through the application of Differential Evolution (DE), a type of Genetic Algorithm. DE is used to optimize the parameters of the UXO fundamental mode model to produce a match between modeled response and the measured response of an unknown object. When this optimization procedure is applied across a library of models for possible UXO, the correct identity of the unknown object can be ascertained because the corresponding library member will produce the closest match. Furthermore, responses from clutter objects are shown to produce very poor matches to library objects, thus providing a method to discriminate UXO from clutter. These optimization experiments are conducted on measurements of UXO in air, UXO in air but obscured by clutter fragments, buried UXO, and buried UXO obscured by clutter fragments. It is shown that the optimization procedure is successful for shallow buried objects obscured by light clutter contributing to roughly 20 dB SNR, but is limited in applicability towards very deeply buried UXO or those in dense clutter environments. The general conclusion forwarded by this work is that while increasingly accurate discrimination capabilities can be produced through accurate forward modeling and application of robust optimization and learning algorithms, the presence of noise and clutter is still of great concern. Minimization or filtering of such noise is necessary before field deployable discrimination techniques can be realized.

I. Introduction

Electromagnetic techniques have a long history of application in remote sensing and detection of obscured targets. When a time varying electromagnetic field interacts with a conducting body, electric currents will be induced on the target. As an example, in a typical EMI response of a metal object to a uniform excitation, the object is a permeable sphere with $\sigma = 2\times106$ S/m, radius a = 0.05 m, and $\mu = 100\times\mu0$. “I” denotes the response that is in phase with the excitation and “Q” denotes the response that is in phase quadrature with the excitation. I and Q correspond to the real and imaginary parts of the secondary field, respectively. In the geophysics convention, the I term is always plotted so that its sign is reversed. The trends and characteristics can be more easily understood by examining the high and low frequency limits. At near static frequencies, the response is mainly due to the magnetic polarizability of the object. The response will align itself with the incident magnetic field and be wholly Inphase. If the object were not permeable, very little response would be seen at the low frequency end of the EMI spectrum. At the highest frequencies, activity will be largely limited to surface currents that generate an opposing response as stated by Lenz’s law and again will be entirely Inphase but of opposite sign. At mid-frequencies, the finite conductivity of the target provides resistance as volume currents circulate within the target in their attempt to oppose changes in the primary field. Therefore, the secondary magnetic fields produced by these currents will lag behind the incident magnetic field and produce a quadrature response.

II. UXO, Soil, and Sensor Modeling

The goal of reducing false alarms can be addressed by identifying or classifying buried objects based on their EMI response. However, to perform such discrimination, forward models are needed beforehand to predict the secondary magnetic fields produced by targets under various conditions. Many inversion techniques require some prior knowledge of the target’s response under specific conditions. Normally, it is not financially or logistically feasible to take measurements of UXO or related targets for every orientation and position of interest. Therefore, forward models form an integral part of inversion research. Furthermore, accurate forward models of UXO or similarly shaped metal objects form a critical part of the understanding of their response to EMI stimuli. What largely distinguishes the work discussed here from all previous forward modeling work is the attention to modeling UXO within realistic environments and using real instruments. This complete model consolidates the effects of soil and the effect of the relationship between actual secondary EMI fields and the measured fields as reported by the sensor. All previous modeling work was limited to modeling targets in free space. Accurate modeling of the measured EMI response of buried UXO in realistic environments is comprised of three key components: the UXO itself, the soil, and the sensor in use.

The spheroidal mode model for UXO is a natural extension of the prior research into retrieving spheroidal mode coefficients from data and is similar in structure to the fundamental mode model. It must be emphasized that the spheroidal mode model is distinct from the spheroid model. The spheroid model is analytical and only models spheroids. The spheroidal mode model–though drawn from the analytical framework of the magnetic response in the spheroidal coordinate system–is similar to the fundamental mode model in that its parameters are obtained from EMI measurement data and can model metal objects of any shape provided sufficient measurements are available. Whereas the fundamental mode model describes objects using sets of magnetic charges, the spheroidal model utilizes the coefficients of the spheroidal modes of the target's response.

III. Inversion through Application of Differential Evolution:

Identification

Predicting the output of a system given specific input values requires a model that follows some basic underlying laws governing the system. This prediction constitutes the "forward problem." Conversely, the "inverse problem" attempts to recover the input values when given the response of a system. The forward problem in regards to UXO research can be resolved with accurate modeling of UXO objects and the environment. Several reliable forward models have been developed and are readily available. That aspect of UXO research is relatively mature. However, the inverse problem of identifying UXO objects through their EMI responses is a topic currently of great interest. There are several approaches to general inverse problems. If the system can be described by a set of linear equations, the input parameters can be solved when given sufficient output data. If the system is non-linear but characterized by a closed form expression, the inverse problem can often be solved through various calculation techniques such as the Gauss- Newton algorithm. However, given the complexity of the UXO problem where the target is often buried at an unknown location, depth, and orientation, no closed form expression can completely describe the entirety of the system.

The inverse problem for UXO encompasses two general forms. The first form uses the EMI response signal to resolves identity of the target from a library standard, representative UXO types. Items whose identities cannot be resolved are then considered clutter items. The second form of inversion does not identify particular UXO but makes a general discrimination between all UXO targets and clutter. One can view the object identification problem as a type of optimization problem. Optimization describes a process where one searches for the optimal values of a model's input so that the model's output will correctly match given data. Cast in terms of the UXO problem, optimization requires measuring the EMI response of the

unknown target in question and comparing this signature to the predicted responses from a library of models for possible UXO targets. The input parameters of the models are adjusted until the "best" match, as evaluated by an objective function, is achieved. The member of the library which produces the closest match with an acceptable level of accordance will correspond to the identity of the unknown object. There are three basic components of the optimization inversion scheme: the model, the search algorithm, and the objective function. Each component has the potential of rendering the optimization unsuccessful and must be thoroughly evaluated and tested:

1. The Model: To make the calculation tractable, the model must be computationally fast because the optimization process will require many evaluations over the course of the search process to find the most optimal input parameters. The fundamental mode model and the spheroidal mode model are both analytical models which only involve the summation of a finite number of response components, represented as magnetic charges or Bjk modes respectively, and do not involve inverting large matrices. Therefore, both are comparably fast and suitable for use in an optimization scheme. However, as will be discussed, due to the differences in the specific implementation structure of each model, the fundamental mode model is favored because it can accommodate a faster search method.

2. The Search Algorithm: The process of searching and adjusting the input parameters until a good match between modeled response and data is found requires multiple evaluations by the model. Any actual buried UXO will be at an unknown position and orientation underneath the soil. Therefore the search process involves checking combinations of position and orientation–which are the only inputs of the fundamental mode model–for each library member until the best match is obtained. An exhaustive brute force search would not be feasible even for a relatively fast model such as the fundamental mode model. As will be discussed, this study employs differential evolution (DE), a type of genetic algorithm, as an effective search strategy. However, despite the improvement over a brute force method, DE still requires considerable computational time. To counter this deficiency, the DE computation is parallelized using Message Passing Protocol (MPI).

3. The Objective Function: Since the optimization procedure searches for the best match between model output and measurement data, some quantitative measure of "goodness of fit" is required. Normally this measure is an analytical expression for the difference between the model output and data. This expression is called the "objective function." We give the description of the weighted, normalized difference used to calculate error in this study.

In response to the need for a search algorithm in the optimization scheme, this study implemented a differential evolution (DE), a type of genetic algorithm. Genetic algorithms describe a family of algorithms which employ evolution strategy optimization. This form of optimization is based on the genetic mechanisms and

evolution in biology. Many possible solutions to the problem of interest are evaluated by how well they solve the problem. Good solutions are allowed to remain while poor solutions are discarded. This selective process parallels the idea of evolution which mandates the “survival of the fittest” for individuals within a population inhabiting a hostile environment. Very fit individuals are also likely to have fit offspring in the next generation due to passing on favorable genes. The genes of the offspring are similar to but slightly modified from the genes of the parents as governed by the known genetic mechanisms of crossover and mutation. This slight change has the potential of improving the genes which may be passed on to the next generation and so on. This process is mirrored in genetic algorithms. An individual is now a solution to the problem of interest. The population therefore is a finite collection of possible solutions. Instead of a hostile environment determining the likelihood of survival, a solution’s “fitness” is measured by how well it solves the problem at hand. Solutions are culled when they under perform. “Generation” in computational terms refers to a complete cycle of evaluation for all the solutions by the objective function. Instead of reproduction, new solutions are generated to be slightly altered versions of the good solutions belonging the previous generation. In subsequent generations, these slight changes should allow the solutions to converge upon the best possible solution. Genetic algorithms have been used to facilitate searches and provide optimal solutions to non-linear problems.

Differential evolution is a type of genetic algorithm largely distinguished by its use of vector differences of randomly selected population members to perturb the current population and produce the subsequent generation. Another aspect of DE is that it is very well suited for parallelization since each member of a population can be evaluated independently with regards to whether it should be replaced or be allowed to remain in the subsequent generation. This flexibility allows for decreased calculation time without the loss of the ability to converge on the most optimal solution. Like all genetic algorithms, DE is very computationally expensive. Given the current state of computing power, inversion is very time consuming unless the DE algorithm is parallelized, using such methods as the Message Passing Interface (MPI) protocol, and run on a supercomputer. For this investigation, the US Army Research Laboratory’s High Performance computing center’s Cray supercomputers with MPI-compatible software was used to perform the DE optimization.

The objective function is a measure of how well a proposed solution satisfies the problem of interest. Various objective functions have been proposed and used in inversion research. For the UXO inversion problem, the objective function must compare simulated EMI responses Hx, fm created by a model to measured “data” EMI signals Hx, fd where each signal provides a sampling of the secondary magnetic field at Nx observation positions indexed by x and Nf frequencies indexed by f. Given the variability of the signal’s amplitude across space and frequency, a simple difference, normalized by the number of samples, between the two signals offers an incomplete picture of how well these two signals correspond.

Signals differences arising stronger signal samplings will dominate the calculated error. To demonstrate the inaccuracy of this object function, one can imagine obtaining measurements of a UXO at two elevation planes. The upper elevation plane would measure weaker signals. Differences between weaker signals would be smaller than differences between stronger signals. Therefore, the final calculated error would be incorrectly biased towards lower values. To prevent this bias, the difference must be point-wise normalized by the magnitude of the data such that the difference at any sample point becomes a percentage of the signal at the same sample point.

DE requires multiple, successive evaluations of the forward model. Therefore, it is advantageous to select the fastest model of acceptable accuracy. The fundamental mode model and the spheroidal mode model are both comparably fast given that both compute responses as a sum of a finite number of modes derived from stored values. However, the fundamental mode model is implemented in FORTRAN while the spheroidal mode model is written in Matlab. This difference is critical due to the lack of Matlab-based MPI capabilities at the Army Research Laboratory High Performance Computing facility which provided the parallelized processors. Therefore, the fundamental mode model is used as the forward model in this portion of the inversion study.

It should be noted that the fundamental mode model was derived from GEM-3 measurements of actual UXO. The values of the magnetic charges which characterize the response of an object in this model reflect the units by which the GEM-3 reports all measurement data. Any prediction made by the fundamental mode model has the same units as all measurements outputted by the GEM-3. Therefore, the application of the scaling factor to ensure consistency between forward model and measurements is not needed. The scaling factor, however, must be applied whenever a wholly analytical forward model, such as the spheroid model, is in use. This scenario corresponds to the research into UXO classification.

Because the FORTRAN source code for the fundamental mode model is available, DE is written into this code to provide full integration and therefore eliminate any associated communication latency which would contribute to a slower performance.

The fundamental mode model was previously shown to provide predictions for specific UXO types. Therefore, it may be more accurate to refer to the fundamental model as a library of specific UXO models. Of the available UXO types within the model, four are selected to form this library and to be used as part of the optimization scheme. In each test case, described in the subsequent sections, either only one or none of the library members correctly corresponds to the unknown target. For each UXO type within the fundamental mode model, only the orientation and position of the object is needed as input. Therefore, for each object in the library, DE will recover the (x, y, z) position and (θ, φ) orientation that will create the best match to the signal

from an unknown target. The library object which has the closest match is then taken to be the identity of the unknown object.

Given that the search parameters are (x, y, z) and (θ, φ) for each library member, each candidate in the population is of vector of length 5. References state a population size should be roughly 10 or more times the number of search parameters. The forward model will be extended to include soil half space effects. Soil permeability μ will form the sixth input parameter into the model. Therefore, for all work presented here, a population size of 60 is used.

DE also requires the user to specify the bounds of each search parameters. The inclination parameter θ which specifies the angle from the positive z axis to the $x - y$ plane is allowed to vary from 0 to π. The rotation angle, φ, varies from 0 to 2π. In the simulation, x and y spans from -0.3 m to 0.3 m. The sensor is located on the $z = 0$ plane or above. The depth of the target's center, z, spans from -0.1 m to -0.7 m. Candidate solutions whose parameters create a non-physical possibility, such as the UXO intersecting the measurement plane, are explicitly rejected. These parameters are first initialized randomly with values drawn from their permitted ranges.

A larger F indicates a more aggressive change and produces a faster but less robust solver. A smaller F indicates a more gradual change producing a slower but more robust solver. Through trial and error, it was found that the use of $F = 0.4$ provides the most consistent, correct convergence. Some literatures suggest using crossover and mutation, "M", to complement the differential change. While this study implemented these additions, no appreciable difference was observed when these features were added to DE. Therefore, all results were created without the use of crossover and mutation.

The population size in use determines the number of processors MPI divides the work across. Each processor is assigned to one population member so 60 processors are used in parallel. In addition, one more processor must be used for the controlling and aggregating process. Since DE is implemented in FORTRAN and integrated into the source code of the fundamental mode model, the MPI FORTRAN commands are likewise inserted into this code.

The following inversion results present four basic cases, each progressively more difficult:

1. Inversion for a target in free space;
2. Inversion for a buried target;
3. Inversion for a target underneath clutter in free space;
4. Inversion for a buried target underneath clutter;

In each case, models are first used to produce synthetic data. This synthetic data is then used by the inversion algorithm to determine the identity of the target and ascertain any limitations on accuracy of the inversion. After the synthetic data study,

corresponding measurements of the target are taken and processed by the inversion algorithm in a likewise manner.

As the first test for a target in free space, only synthetic data is used. The model's output is matched with outputs previously generated. This test allows the verification of the capability of the DE algorithm and the selected objective function. In all tests, the measurements and calculated responses were on a 7 by 7 grid of 10cm spacing. For synthetic data, the plane was 0.35 meters above the center of the object. The synthetic data are generated by the fundamental mode model with input parameters x = 0.1m, y = 0.1m, z = 0.35m, $\theta = 3\pi/4$, and $\varphi = \pi/2$.

For this test, the DE algorithm uses 50 members in the population and runs for 100 generations. The true and recovered position and orientation values for object ATC188 deviates roughly 1 cm away from the true position. Given that this object is more than half a meter in length, this deviation is comparatively small. One can also examine the convergence of the DE algorithm through successive generations.

The F value of 0.4 used in the previous example provides the most suitable balance between correct convergence and speed. A faster convergence would mean fewer generations and thus faster running times. However, increasing the F value can lead to improper convergence where the optimized (x, y, z, θ, φ) values are much less accurate. This inaccuracy and improper convergence can be shown by examining objective function. Here, F = 0.7. While DE converges rapidly, it converges on a solution which has a much higher error than that created when F = 0.4.

The above analysis can be extended to a large range of targets. First, the fundamental mode forward model generates responses for the four members of the library. Using these modeled response, DE recovers the orientation and location of each member of the library that will produce the best match to the data. In addition to confirming the applicability of DE and the selected objective function, this test will also specify the lower bound on error. Any error will be inherent to the DE method and will not be due to any inaccuracy of the forward model or measurement noise. As stated earlier, this error can be thought of as a percentage of the mean of the overall response. The rows correspond to data generated from the model for each particular UXO. The columns correspond to the candidates in the library. The diagonal values correspond to the correct match between object producing the synthetic data and the library member. Therefore, the low error values on the diagonal are the lowest in their respective row and demonstrate that identification of UXO is achievable with DE.

As a first step in using real data, DE is used to match measurements of a known object with its corresponding model. Measurements are taken of object ATC188 in free space on a 7 by 7 grid with 10cm spacing. The measurement plane is 15 cm above the nearest point in the object. The object is roughly at the center of the grid and has a θ value of about $\pi/2$. Given the impreciseness of measuring the UXO

position, the object's exact position and orientation are unknown and must be retrieved as part of the inversion process. One can show the goodness of fit between the output of the optimized forward model for ATC188 and measured data. This match produces an error of 0.08 as measured by the objective function.

The previous DE inversion results are for objects measured in a laboratory environment where free space is a good approximation for the background medium. Inversion of a UXO buried in soil is considerably more difficult due to the environmental noise. And as shown previously, a half space will create an offset in the Inphase portion of the EMI response which must be taken into account during the inversion process.

Accounting for soil offset within the inversion process may be done in two ways. The first method involves removing the effect of the soil offset from the data prior to inversion. This may be done by taking measurements of nearby soil that do not contain UXO targets and then subtracting that data from the measurements of the buried UXO. This technique, however, requires access to "uncontaminated" soil that has the same material properties as the soil containing UXO. Furthermore, the unevenness of the surface of the soil will create varying distances between sensor and the surface. In measurements this variation will manifest itself as noise. Therefore, a smooth soil surface is desired in all measurement. While these conditions can be reproduced in controlled environments, the same cannot be said of all real UXO recovery scenarios.

The second method to account for the present of soil is to invert for the soil properties within the overall UXO inversion scheme. Much like how DE recovers an object's position and orientation in the optimization process, DE can also recover a soil's permeability value. A half space response can be added to the fundamental mode forward model. Given known transmitter characteristics and elevation, this half space response can be determined by a single μ parameter. Therefore, as part of the optimization process, μ must be explicitly recovered along with (x, y, z) and (θ, φ). For the analysis of synthetic data created by modeling UXO in permeable backgrounds, the second method to account for soil is applied.

IV. Effect of Clutter on Differential Evolution Inversion

Another large contributor to noise is the presence of very small diffuse metal clutter objects, often very near the surface of the soil. While these clutter items are much smaller than the large discrete clutter, small diffuse clutter may still create a very strong EMI responses when the sensor passes above. Therefore, the impact of diffuse clutter pieces on the overall EMI response of buried UXO must be taken into account. This study first examines the effect of modeled small clutter in the inversion of synthetic data before proceeding to measurements of UXO overlaid with clutter.

Small pieces of clutter can be modeled as dipoles and their combined response can be superimposed onto a UXO forward model prediction of the secondary field. This superposition creates a model for a UXO obscured by clutter. The modeled clutter is comprised of 20 dipoles, characterized by a magnetic polarizability matrix of a metal sphere in a uniform field. These dipoles are randomly dispersed over an area of 0.6 by 0.6 meters and a depth of up to 0.5 meters, corresponding to the allowable range for the position of the modeled UXO target. The spheres ranged in size from 0.5cm to 2cm and have material properties equal to either typical steel ($\mu_r = 100$ with $\sigma = 2 \cdot 106$ S/m) or typical aluminum ($\mu_r = 1$ with $\sigma = 2 \cdot 107$ S/m). The presence of these spheres creates a level of noise that is comparable to about 19dB SNR.

The 5 parameter DE optimization is used to recover $(x, y, z, \theta, \varphi)$ for each library member. DE matches the forward models to the noise corrupted signatures of the targets, identifying the best matching object amongst the candidates in the library. This inversion uses a 50 member population, running for 100 generations. The correct library member still produces the lowest error in each row. However, as one might expect, the errors are larger than in previous examples where no clutter was present in the synthetic data.

V. Inversion through Application of Machine Learning: Classification

While DE inversion is shown to be capable of recovering the identity of buried targets when given a library of candidates, that technique is hampered by the computational requirements. Despite use of parallelization and access to supercomputers, processing requires at least a few hours. Given current computing limitations, DE is therefore not a suitable method for real time, on-site inversion. While computational power is steadily increasing with time, there is always motivation to obtain a faster solution that may be obtained within the confines of the present computing capability. Furthermore, the DE method requires compiling a library of specific possible objects and has difficulty generalizing for UXO objects not included in the library because the optimization procedure produces similar levels for goodness of fit between disparate objects. A UXO not in the library would go unrecognized. Therefore, an alternative method to pursue is to discriminate all UXO from clutter generically, as opposed to identifying particular UXO or UXO types. The inversion problem can be considered as a classification problem: given the EMI response of an unknown object, one must classify the object as either a UXO or a piece of clutter.

To form such a discriminator, several topics must be investigated:

1. What characteristics distinguish UXO from clutter objects? The most basic question one can ask is how UXO can be physically distinguished from clutter objects. To that end, the following section will discuss four basic physical characteristics of UXO not found in typical clutter.

2. How are these physical characteristic represented in the UXO's EMI responses? The physical properties of objects dictate their corresponding EMI response. Therefore, it may be possible to find distinguishable traits or features within these EMI responses that relate to the physical nature of the target.

3. What is the relationship between these features and the physical characteristics of the object? If it is possible to derive distinguishable features of EMI responses which relate to the physical nature of the object, then the next objective would be to decipher such a relationship.

One particular machine learning method, support vector machines, will be introduced and discussed. Once the relationship between Bjk values, characteristics of the target which may be found through the corresponding EMI response, and the physical nature of the targets is known, classification would only require examining the Bjk values of any new target to determine if the object physically is more similar to UXO or to clutter. As discussed earlier, Bjk values may be recovered from any target given enough EMI measurements. Therefore, this method has the potential to classify objects in a real time, on-site process when enough measurement data of the buried target are taken. Therefore, this method has several distinct advantages over DE inversion and warrants investigation.

VI. Determining Clutter and UXO characteristics

To perform discrimination between UXO and clutter, it is necessary to ask what physical characteristics distinguish clutter objects from UXO targets. The earlier discussion on DE inversion included examples with larger clutter objects and sheets of very small diffuse clutter pieces. Large clutter pieces can possibly be mistaken for UXO while small diffuse clutters largely contribute noise to the measured EMI response. Figure 1 shows clutter pieces of various sizes that were recovered from UXO sites. Note both the shape and size of these clutter objects. The largest is around 10cm. The UXO shown in Figure 2 is around 80cm. It is elongated and has a general body of revolution shape. From such inspections, one can decided upon several basic key physical features to distinguish UXO from clutter:

Figure 1: Large discrete clutter objects recovered from UXO sites. Photograph courtesy of CRREL.

1. Body of Revolution (BOR): UXO are almost always a BOR. Even the presence of fins or other small deviations on a UXO does not affect the response of the object to the extent that one is able to distinguish it from true BOR objects. In contrast, clutter can have any random shape.

2. Size: Field workers involved in UXO cleanup are particularly interested in distinguishing larger objects from relatively smaller clutter items. These clutter items can have a strong EMI response if they are buried at shallow depths which is a common scenario. Since the strength of the object's response is a poor indication of the object's size, more sophisticated discrimination processing is necessary to avoid the costly task of digging up these clutter objects.

3. Homogeneity: UXO are usually composed of a number of different materials while clutter, often fragments and casings from exploded ordnances, are often homogeneous.

Realistic obstacles to successful discrimination must be considered when developing any practical classification method. The classification must be general enough to be applied to a wide range of possible objects since there is a substantial

range of possible clutter items and UXO. The classification must be robust enough to be minimally affected by sensor and environmental noise. Furthermore, for real time application, the classification must be fast. All of these points are addressed in this research.

Figure 2: Typical UXO object. Photograph courtesy of CRREL

VII. Selection of Feature Vector: Distinguishable Parameters of EMI Responses

While the DE inversion study uses the EMI response of objects directly, these responses are highly dependent on target's orientation, location, and sensor in use.

One would like to find features of the EMI response which only relate to the physical nature of the object. These features may offer clues to the object's generic characteristics, such as size, shape, and symmetry, which may strongly indicate whether the object is a UXO or clutter. One such feature came to light as the result of previous work in developing the spheroidal mode forward model within the spheroidal coordinate system. As discussed, within this coordinate system, the excitation and response of a UXO or any other object can be described in terms of scalar spheroidal modes consisting of associated Legendre functions. The spheroidal response modes each have a coefficient Bjk which correspond to the kth mode of the spheroidal response due to the jth mode of the spheroidal excitation. The Bjk have been proven to be unique properties of an object in the sense that objects producing different scattered fields must have different Bjk. For a coordinate system aligned and centered on the target, Bjk are completely independent of the excitation, orientation, and location of the object. Thus Bjk values only depend on the physical properties of the object. Consequently, these Bjk coefficients, which can be recovered from the measured signal, are appropriate inputs into classification algorithms.

Methodology

The study of using machine learning algorithms to infer an object's physical properties from associated Bjk values of their response has four major steps to be discussed in the subsequent sections:

1. Creation of Training Data: SVM requires the Bjk values of a large set of representative objects to form the training data. A large set is required to ensure that the trained SVM can generalize for all objects one may encounter. A forward model must be used to create this training data because is not normally possible to find and measure enough objects to create training data composed solely of real targets. Of the forward models available, the spheroid model is most suitable for the creation of the training data because it can predict the response of any arbitrary shaped spheroid target of any σ and μ value. This flexibility ensures the training data will be broad and encompass many dissimilarly shaped objects.

2. Creation of Test Data: Unlike training data, test data need not be numerous and may be taken from forward models or from measurements. Synthetic test data, from forward models, may also include additive noise factors or other uncertainties which model the noise seen in measurement data.

3. Obtaining Bjk Values: All synthetic data and measurement data are comprised of magnetic fields at various sensor locations. To form the appropriate inputs into the learning machines, the Bjk values pertaining to the target must be extracted from these magnetic fields.

4. Examining Accuracy of Trained Learning Machines: Once the Bjk values for

the training data are obtained, the learning machines can be trained. Their level of error in classifying the test data will determine the ability of the learning machines to distinguish between objects with qualities similar to UXO from those with qualities unlike UXO. The effect of noise on classification accuracy is also investigated.

Object Modeling and Composition

This investigation uses three different object types. First, the simplest object is a single spheroid as shown in Figure 3(a). The spheroid has two possible permeability and conductivity values: either $\mu_r = 100$ with $\sigma = 2 \cdot 106$ S/m or $\mu_r = 1$ with $\sigma = 2 \cdot 107$ S/m. These values approximate steel and aluminum, two metals commonly present in UXO and clutter. The elongation of each spheroid, the ratio of major axis length to minor axis length, is taken from a uniform distribution ranging from 0.1 to 4. The volume is likewise random and uniformly distributed, ranging from 0.001 m3 to 0.08 m3. 0.04 m3 is the cutoff between “large” and “small” objects. This range of values corresponds to the variety of UXO and clutter objects one would expect to encounter in the field. If different ranges of volumes are of interest, new training data can be created and the learning algorithms can be retrained to recognize different cutoff values. These spheroids are modeled using the spheroid model. The main difficulty in the generation of synthetic data is the amount of time needed to create enough objects for the training set. To generate data for 1800 objects, around two days are needed on a 3.6 GHz Pentium 4 PC. While the computational time is substantial, the creation of the training data occurs infrequently: once a learning method is trained using a training data set, it may be repeatedly used to classify any object without requiring any further significant calculation. In this regard, classification by machine learning is much faster than identification by optimization which must proceed through the entire lengthy optimization process for every measurement with every library member.

The second type of object one can model is a heterogeneous object composed of two small spheroids that are coaxial and are separated by a distance of 1 mm as shown in Figure 3(b). Thus the object is a body of revolution (BOR). Since it is composed of two different materials, it is referred to as a BOR composite object. This object is always positioned so that the gap is fixed at the center of the coordinate system. The two spheroids that form a composite object are always given two different permeability and conductivity values: $\mu_r = 100$ with $\sigma = 2 \cdot 106$ S/m and $\mu_r = 1$ with $\sigma = 2 \cdot 107$ S/m . The elongation of each spheroid is again random. The total volume of both spheroids ranges from 0.001 m3 to 0.08 m3. To obtain the response of a composite object, the magnetic field response of each spheroid is independently calculated and then summed. This study assumes that the interaction between the two

spheroids does not affect the fields at the observation points which are at least a characteristic length away. As mentioned earlier, prior research has shown that this is a reasonable assumption even for closely spaced objects as long as one object is not permeable and the observation point is more than one characteristic object length away.

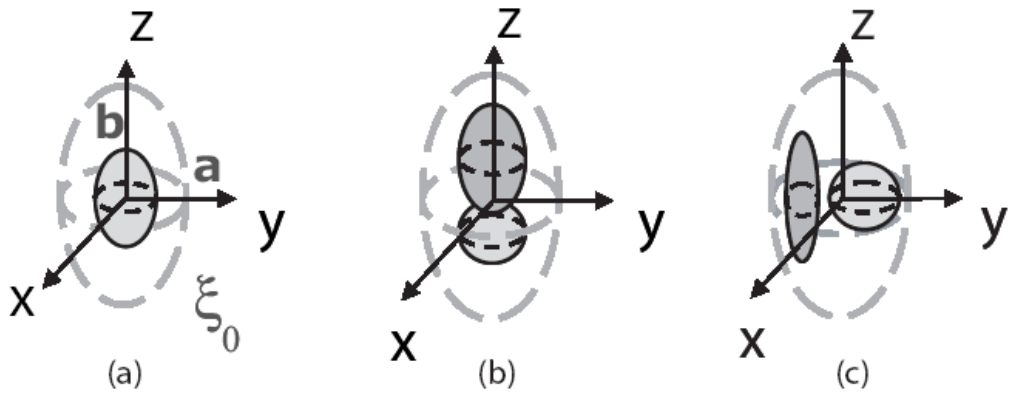

Figure 3: Three different configurations of spheroids: single, BOR composite, and non BOR composite. The Bjk of these three objects are used for SVM and NN training and testing.

The third type of object under study is shown in Figure 3(c). This object is similar to the BOR composite object except now the axes are parallel to each other and the z-axis. The gap between the two spheroids is again 1 mm and is positioned at the center of the coordinate system. This object is referred to as a non-BOR composite object. The excitation calculated by the model of the GEM-3 sensor is validated and shown to be faster than other methods. The GEM-3 instrument, the primary tool to produce EMI measurements, is manufactured by Geophex. As mentioned earlier, this instrument consists of two current loops in a bucking coil arrangement to generated primary magnetic field. The secondary magnetic field is captured by the current generated on a pickup coil in the center of the instrument by $\partial B/\partial t$. However, the instrument reports this current in units that is proportional to the integral of magnetic flux over the receiver coil through a division by $i\omega$ of the receiver coil current as implemented in hardware and post-processing.

Retrieval of Bjk from Magnetic Fields

For the training data and some of the test data, the Bjk are recovered from magnetic fields generated from a forward model. The magnetic fields are sampled at 578 points in space, thus ensuring the problem is over determined. These points were distributed over a 2 m by 2 m grid at two elevations, 1.1 m and 1.3 m from the center of the spheroid. Figure 4 gives a graphical depiction of this arrangement. As before, only the lowest order modes are used, and they correspond to j = (0,0,1), (0,0,2), (0,1,1), (1,1,1), (0,0,3), (0,1,2), (1,1,2) and k = (0,0,0), (0,1,1), (1,1,1), (0,0,1), giving a total of 28 Bjk coefficients. Previous work demonstrated that these low order modes

dominate the solution and are sufficient to reproduce it. The modes (0, 1, 1), (1, 1, 1), and (0, 0, 1) for k correspond to the magnetic dipole moments in x, y, and z directions for each excitation mode. Thus for each j, we are only solving for one more mode in addition to the three modes which correspond to the tri-axial dipole moments. Each Bjk is a complex value. But due to the limitations of the SVM algorithm, the real and imaginary parts are considered independent inputs when processing. For each object, we consider the Bjk at two frequencies: one high at 10950 Hz and one low at 210 Hz. This choice of frequencies is due to the nature of the EMI response: these frequency extremes can capture the largest variation in an object's Inphase frequency response. Consequently, a vector of total length n = 112 serves as input for each object into the machine learning algorithm.

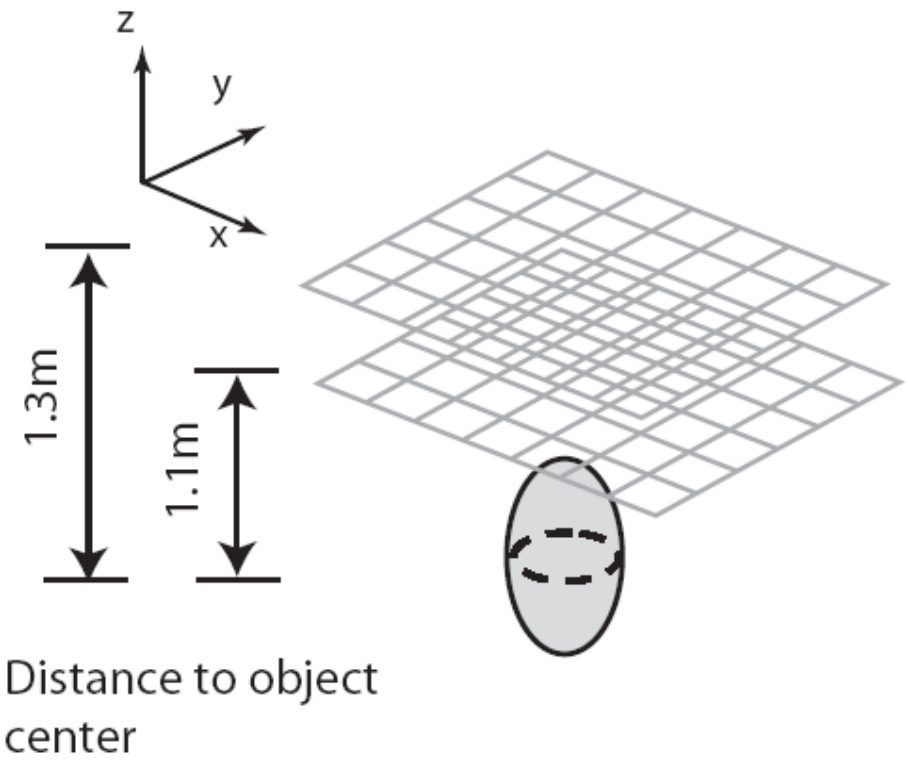

Figure 4: Diagram of the measurement locations used in the inversion process.

VIII. SVM Classification Results

Large vs Small

For all tests, the training data is a set of 1800 objects that are evenly divided into the two possible classes of large and small. The test data set has 200 members and is generated independently from the training data set. Adequate classification can be achieved with as few as 600 training examples for the simple case of single spheroid test objects with no additive noise. However, past experience demonstrate that the

more complex objects presented in the subsequent sections require larger training sets to be optimally classified. Therefore, to permit reasonable comparison of the classification performance for different objects, all training sets have 1800 members. Many classification studies employ small training sets and larger test sets because the training set often derived from measurements and collected data are difficult to obtain. However, the forward model can provide large amounts of training data within a reasonable amount of time so larger training sets are used. In the first test, when single objects are classified by a trained SVM, only 2 objects are misclassified. Table 1 is the confusion matrix that of the result of classifying the test data. SVM misclassifies 2 objects out of a total of 200, yielding an error of 1%. This error is used as the overall figure of merit as opposed to separate false positive and false negative rates. The errors made by SVM are concentrated close to the boundary between "large" and "small." While the clustering of markers suggests some correlation between object size and overall Bjk magnitude, the relationship is not strict as we have discussed earlier. One can clearly see many large objects with lower Bjk than smaller objects and visa versa. Table 1 shows how SVM is able to generalize for different types of objects. There are three sets of test data and three sets of training data. All cases use 200 test objects and 1800 training objects. The lowest errors are generated when we train and test using the same type of object. When SVM is trained on single spheroids and tested on BOR composite objects or visa versa, it is able to generalize across these two object types to a certain degree. But it has difficulty classifying non-BOR objects when trained on any of the other two types or visa versa. In many cases an exact 50% error is obtained when SVM simply classified all objects as large or all objects as small. This unsuccessful classification may be due to the peculiarity of BOR objects in that they have values of zero for many specific Bjk coefficients while non-BOR objects do not have this constraint. Due to this very distinct difference in pattern, we expect SVM to have greater difficulty when generalizing across BOR and non-BOR objects. However, when SVM is given sufficient training data, it can adequately classify all objects. Table 2 shows the effects of training on a combination of single and BOR composite objects and a combination of all three types of objects. Remarkably, training on a combination of BOR composite and single objects allows SVM to be even more accurate in classifying BOR type objects. Furthermore, training with all three object types creates a more general SVM that can classify all objects with under 5% error. For any classification technique to be of practical use, it must be able to generalize for a wide range of objects. Thus, this use of dissimilar training and testing objects characterizes the generalizability of each trained learning method. Furthermore, mixed training sets, comprised of two or more types of objects, helps to illustrate how broadening the scope of the training sets improves generalizability and leads to overall robustness.

	Train: Single (BOR)	Train: Compos-ite (BOR)	Train: Composite (non-BOR)
Test: Single	1.00%	24.0%	50.0%
Test: Composite (BOR)	18.5%	3.00%	47.5%
Test: Composite (non-BOR)	50.0%	50.0%	1.50%

Table 1: Table of Error for SVM Classification with Different Training and Testing Sets

	Train: Single and Composite (BOR)	Train: All Three Types
Test: Single	1.00%	2.50%
Test: Composite (BOR)	0.00%	4.50%
Test: Composite (non-BOR)	50.0%	4.50%

Table 2: Table of Error for SVM Classification with Mixed Training Sets

SVM Results with Measurements

The SVM classification is then tested using data from measured objects. The largest clutter item has a volume of 53 cubic centimeters. The largest UXO has a volume of roughly 2000 cubic cm while the smallest has a volume of about 700 cubic cm. Therefore, a new SVM training set with added Gaussian noise was created where the random spheroids had volumes within the range of 10 cm3 to 2500 cm3 with 300 cm3 as the boundary between small and large. When the trained SVM was presented with Bjk drawn from measurements of these four objects, it correctly distinguished

the very large objects from the small objects as shown by Table 3.

	True Large (UXO)	True Small (Clutter)
Predicted Large	4	0
Predicted Small	0	4

Table 3: Confusion Matrix for SVM Classification of Clutter Items and UXO

	True BOR	True non-BOR
Predicted BOR	100	0
Predicted nonBOR	0	100

Table 4: Confusion Matrix for SVM Classification of BOR Items and non-BOR Items

Distinguishing BOR composite objects from non-BOR composite objects is another area of investigation. The 1800 member training data has equal parts BOR and non-BOR composite spheroids. When trained on this data, SVM is very accurate in classifying a similarly generated 200 member test set as seen in Table 4. This accuracy is likely due to the distinct and easily distinguishable pattern for the Bjk of BOR objects. In BOR objects, only specific low order Bjk are non-zero

IX. Conclusion

The problem of classification by volumetric size and other physical characteristics of metallic objects using their EMI response are solved by decomposing that response into Bjk coefficients and then using a SVM and a NN to process those coefficients. The performance of each method is compared. Since one can demonstrate that there is no simple relationship between sizes of objects and the overall magnitude of their Bjk coefficients and magnetic polarizabilities, learning algorithms may be useful in classifying these objects. Furthermore, both learning algorithms are able to generalize for different object types with varying degrees of success. Both algorithms are capable of classifying single objects when trained on BOR composite objects or visa versa. However, both have difficulty classifying non-BOR objects when trained on any of the other two types or visa versa. One can hypothesize that this increased error is due to the single spheroid also being BOR so the non-BOR objects are very different from the other two types. When trained on all three types of objects, both the NN and the SVM are able to classify all objects with a good degree of accuracy. Furthermore, screening out non-BOR objects from BOR objects can be done with high accuracy so that, theoretically, classification based on size need not encompass both BOR and non-BOR objects. Some investigation is also

conducted in classification by object heterogeneity or BOR characteristics with encouraging results. One aspect of machine learning which has not been included in this study is the topic of feature selection. The 28 low order Bjk at two selected frequencies are an educated guess for which Bjk are the most significant in classification. However, there may be more optimal subset of these Bjk values at the currently used frequencies or other frequencies which serve as better inputs into learning machines. This facet of machine learning research is called “feature selection” and may be a possible area for future work. Furthermore, there is a possibility of developing this technique into a real time application. Training each learning method is not instantaneous but still within the realm of being practical. Once a learning algorithm is trained, it can be used for an extended period of time until the user feels more accurate training data is available. Therefore training need only be a rare occurrence. Generating synthetic training data is the most time consuming part of our research, but this data can be stored and used as long as the researcher deems the training data to be valid. The actual classification of test data by SVM or NN is nearly instantaneous. Solving for the appropriate Bjk from measurements is also nearly instantaneous. Therefore, classification of a buried object as UXO or a piece of clutter can theoretically be obtained as quickly as the EMI measurements can be completed when the object position and orientation are known or are estimated within bounds such as those indicated earlier. In addition, both methods show an ability to generalize for noisy test data when trained with noisy data. This noise can be in the form of additive Gaussian noise or small variations in the position or orientation of the objects relative to the coordinate system. Training on noisy data helps to increase the accuracy of both learning algorithms when classifying objects with noisy Bjk. In the analysis on the effects of uncertainty in object position and orientation, one can see that large deviations in an object’s depth can significantly decrease the SVM classification accuracy. Since accuracy with noisy measured data is very critical for any classification method to be viable in the field, one can conclude that training must always be done using data with added noise and uncertainty to help increase the robustness of the classification method. However, this classification method and the DE optimization method have limitations in regards to the level of noise in the EMI responses. Various clutter suppression or signal separation methods have been advanced. Integrating such methods into these inversion algorithms will further the work in realizing a practical, field deployable solution to the difficult problem of UXO inversion.

Publications

B. E. Barrowes, K. O'Neill, T. M. Grzegorczyk, X. Chen, and J. A. Kong. Broadband electromagnetic induction solution for a conducting and permeable spheroid. IEEE Transactions on Geoscience and Remote Sensing, 42:2479–2489, November 2004.

X. Chen, K. O'Neill, T. M. Grzegorczyk, and J. A. Kong. Spheroidal mode approach for the characterization of metallic objects using electromagnetic induction. IEEE Transactions on Geoscience and Remote Sensing, 45(3):697–706, March 2007.

B. Zhang, K. O'Neill, T. M. Grzegorczyk, and J. A. Kong. Environmental effects on UWB electromagnetic induction inversion techniques and forward modeling of unexploded ordnance. page 127, Cambridge, Massachusetts, March 2006. Progress in Electromagnetic Research Symposium (PIERS).

B. Zhang, K. O'Neill, T. M. Grzegorczyk, and J. A. Kong. Use of EMI response coefficients from spheroidal excitation and scattering modes to classify objects via SVM. volume 6217. SPIE, April 2006.

B. Zhang, K. O'Neill, T. M. Grzegorczyk, and J. A. Kong. Support vector machine and neural network classification of metallic objects using coefficients of the spheroidal mqs response modes. IEEE Transactions on Geoscience and Remote Sensing, 46(1):159–171, January 2008.

Tomasz M. Grzegorczyk, Beijia Zhang, Jin Au Kong, Benjamin E. Barrowes, and Kevin O'Neill, Electromagnetic induction from highly permeable and conductive ellipsoids under arbitrary excitation -- Application to the detection of unexploded ordnances, IEEE Transactions on Geoscience and Remote Sensing, vol. 46, no. 4, part 2, page(s) 1164-1176, April, 2008.